original article

Kinetic and isotherm studies of humic acid adsorption onto iron oxide magnetic nanoparticles in aqueous solutions

Hamzeh Esmaeili, Afshin Ebrahimi[1], Mehdi Hajian[1], Hamid Reza Pourzamani[1]

Department of Environmental Health Engineering, School of Health, Isfahan University of Medical Sciences (IUMS), Isfahan, Iran, [1]Environment Research Center, IUMS, Isfahan, Iran

Address for correspondence:
Dr. Afshin Ebrahimi,
Environment Research Center, Isfahan University of Medical Sciences, Isfahan, Iran.
E-mail: a_ebrahimi@hlth.mui.ac.ir

ABSTRACT

Aims: In this study, humic acid (HA) removal by iron oxide magnetic nanoparticles (IOMNPs) was surveyed in aqueous solutions.

Materials and Methods: Batch adsorption technique was used to determine kinetic and isotherm parameters. The effects of pH value, agitation rate, adsorbent dose, contact times and the adsorbate concentrations on the adsorption efficiency were studied as critical parameters. The IOMNPs was characterized by X-ray diffraction.

Results: HA adsorption on the IOMNPs was fitted with Freundlich isotherm model and followed the pseudo-second-order kinetics. Results revealed that at HA concentration of 10 mg/L, pH 4.5, adsorbent dose of 2.7 g/L, agitation rate of 250 rpm and contact time of 90 min at presence of 0.1 M NaCl as an ionic strength agent, the HA removal reached to about 98%. Also, the turbidity of treated samples was increased with increasing of HA loading.

Conclusions: With increasing HA concentrations, adsorption capacity of IOMNPs was increased and HA removal efficiency was decreased. By adding ionic strength, HA removal was improved and turbidity of treated samples was reduced.

Key words: Adsorption, humic acid, iron oxide magnetic nanoparticles, isotherm, kinetic.

INTRODUCTION

Humic acids (HA) are acidic fraction of humic substances, which found in reservoirs, lakes, groundwater and surface waters, soils and sediments. Average molecular weight of these compounds are about 2000–5000 Dalton and under acidic conditions (pH < 2) are insoluble in water, but are soluble at higher pH values.[1] These compounds have a complex structure, heterogeneous, acidic, mostly aromatic, hydrophobic, contain large numbers of mainly acidic functional groups (e.g., carboxylates, phenolic hydroxyls) and have yellow to black appearance.[2]

They account for a considerable fraction (40–90%) of the dissolved organic matter that is found in all water resources.[3] These compounds are considered as disinfection by-products (DBP_s) precursors and produce the dangerous and carcinogenic organic halogenated substances such as trihalomethanes (THM_s) and haloacetic acids (HAA_s) during water chlorination.[4] HA has adverse effects for the water quality as they have a high tendency to combine with the heavy metals and pesticides and intensify their transportation in water,[5] protect microorganisms against disinfectants, and produce smell, taste and color in water resources.[6]

Access this article online

Quick Response Code:

Website: www.ijehe.org

DOI: 10.4103/2277-9183.100133

This article may be cited as:
Esmaeili H, Ebrahimi A, Hajian M, Pourzamani HR. Kinetic and isotherm studies of humic acid adsorption onto iron oxide magnetic nanoparticles in aqueous solutions. Int J Env Health Eng 2012;1:33.

A variety of treatment techniques have been used to remove these pollutants from contaminated water. Adsorption, among these methods, is an important method, and is currently considered as an high-efficiency removal technique with no harmful by-products production.[3]

In recent years, many adsorbents have been used for removal of HA from water such as husk ash,[5] pillared bentonite,[6] acid-activated Greek bentonite,[3] SiO_2 particles,[7] nano scale zero-valent iron,[8] Kaolin clay,[9] surfactant-modified bentonite,[10] etc. It has been shown that adsorption capacity of iron oxide magnetic nanoparticles (IOMNPs) is higher due to large ratio of surface area to volume and finite size effect.[11] Iron oxides have a high adsorption capacity to adsorb the hydrophobic and acidic natural organic matter (NOM) fractions with larger molecular size such as aromatic portions in humic substances.[12] HA has a high affinity to magnetite mineral particles, especially at lower pH (i.e., pH = 5)[13] and increasing ionic strength, enhances the HA adsorption at each pH due to charge screening.[14]

Because of no necessity to the centrifugation process to separation the IOMNPs from treated samples, compared with non-magnetic adsorbents, IOMNPs are suitable and easily attracted to the magnetic field.[15] Jing-Fuliu *et al.* showed that coating Fe_3O_4 with HA exhibits remarkable enhancement of heavy metal removal efficiency compared with Fe_3O_4 nanoparticles.[16]

The main objective of this study was to investigate the effectiveness of IOMNPs in removing HA from water solutions.

MATERIALS AND METHODS

Preparation of Humic Acid Stock Solutions

HA in its sodium salt was obtained from Aldrich Co., Germany. A weight of 0.1 g of HA powdered was mixed with distilled water in a 250-mL beaker. For better dissolving of HA in solid form, a few drops of NaOH 1 M solution were added. Then, 1000 mg/L stock solution of HA was prepared in a volumetric flask and was stirred for 1 h. The prepared solution was transferred to a dark glass and stored at 4°C.

Adsorbent Characterizations

The IOMNPs (Fe_3O_4) were purchased from Aldrich Co. Table 1 shows certificate analysis of IOMNPs, which was provided from the company catalogue. Also, the inorganic impurities of this product were negligible. X-ray diffraction was carried out to identify component phases and structure of magnetic nanoparticles. Debye–Scherrer equation [Tables 2 and 3] was used to calculate the crystallite sizes of the IOMNPs.[17]

Determination of Point of Zero Charge (pzc)

Batch technique was used to determine the pzc of IOMNPs. The amount of pure adsorbent was added to 50 mL of sodium chloride 0.1 M solution (to maintain the background electrolyte concentration), and initial pH values were adjusted by adding a small amount of NaOH or HCl solutions (0.1 M) from 2 to 12. Then, solutions were stirred at 150 rpm for 48 h and final pH of solutions was measured. All experiments were done at room temperature.

Adsorption Experiments

In present work, batch experiments were used for adsorption studies. To achieve better results, all experiments were carried out in triplicate and blanks were run in parallel. Considered factors in this stage of the work include the pH values (4.5, 6, 7 and 9), HA concentrations (10, 35, 65 and 100 mg/L),

Table 1: Certificate analysis of IOMNPs

Nano powder	Size (nm)	Purity (%)	SSA (m^2/g)	Morphology	Bulk Density (g/cm^3)
Fe_3O_4	60	+99.2	55	spherical	0.84

Table 2: Kinetic, isotherm and determine size of adsorbent equations

adsorption capacity	Equ.1	$q_{t,e} = \frac{(c_0 - c_{t,s})v}{m}$
pseudo-first-order model	Equ.2	$\ln(q_e - q_t) = \ln q_e - k_1$
Pseudo-second-order model	Equ.3	$t/q_t = (1/k_2 q_e^2) + (1/q_e)t$
Intraparticle diffusion model (IDM)	Equ.4	$q_t = k_{int} t^{0.5} + c$
Freundlich isotherm	Equ.5	$\log q_e = \log k_f + \frac{1}{n} \log c_e$
Langmuir isotherm	Equ.6	$\frac{1}{q_e} = \frac{1}{q_{max}} + \frac{1}{k_b q_{max} c_e}$
Debye–Scherrer	Equ.7	$d = (k\lambda/\beta \cos\theta)$

contact times (30, 60 90, and 120 min), dose of adsorbent (2000, 2700, 3400, and 4000 mg/L) and agitation rate (150, 200, 250 and 300 rpm) as critical variables. The optimum value of the above critical variables is the mainly parameter for scale-up and design of economical large-scale devices.

A volume of 50 mL HA solution with defined concentrations was transferred to a 100-mL conical flask. The pH of the samples was adjusted by adding a small amount of 0.1 M HCl and NaOH solutions then; working dose of IOMNPs was added to the solutions. An orbital shaker was employed to shake the mixture. After completion of the agitating process; the HA-adsorbed IOMNPs were isolated from the solutions by a strong magnet (0.7 Tesla). Supernatant solutions were passed through a 0.45 μm filter. Then $UV_{abs\text{-}254}$ was measured by spectrophotometer and its results were reported in cm^{-1}.

In this study, kinetic studies were performed to determine the equilibrium time and reaction order at working concentrations of HA (10, 35, 65 and 100 mg/L) for various periods until adsorption equilibrium was established. Pseudo-first-order and pseudo-second-order models were also compared to find the best fitted one for the experimental data obtained. The best fitted model was chosen based on the higher determination correlation coefficient.

In addition to fit the kinetic data, Intraparticle Diffusion Model (IDM) was employed to interpret the mechanism of adsorption process and determine the rate-limiting step. Weber-Morris equation was used for IDM study.[18]

Adsorption isotherm experiment was used to determine the adsorbed mass of HA per unit mass of adsorbent for HA concentration of 10, 20, 30, 40, 50, 60, 70, 80, 90 and 100 mg/L at optimum conditions. Two important adsorption isotherms, Langmuir and Freundlich isotherms, were used to simulate the experimental data. Linear regression analyses of these models and a comparison of their correlation coefficient, r^2, can be used for selection of the best-fit isotherm. The kinetic, isotherm, adsorbent characterize equations and their parameters are listed in Tables 2 and 3.

To determine the presence of interferences (e.g., colloidal particles, nitrate, nitrite and bromide ions) the UV absorption scan from 200 to 400 nm was used.[19]

Ionic Strength Effect

Similar experiments were carried out in order to determine the effect of ionic strength. NaCl was added to the mixture of HA and IOMNPs and ionic strength was adjusted in the range of 0.005 to 0.1 mol/L. The effect of ion strength on the final produced turbidity also was evaluated.

Instrumentation

The X-ray diffraction pattern (XRD) records were carried out in order to characterize the crystal structure of the IOMNPs using a XRD D8 advance, Bruker, Germany. HA analysis was carried out using a DR-5000 spectrophotometer (HACH LANGE model, USA). Sample solutions pH were measured and adjusted using a pH meter (EUTECH 310, China). An IKA® KS260 orbit shaker, Italy, was used to shake the mixtures. Turbidity of the solutions was measured by a Turbidimeter 2100P HACH model, USA. A magnetic field with strength of 0.7 Tesla was employed for separation of IOMNPs from the mixtures.

RESULTS

Characterizations of IOMNPs

Phase identification of the IOMNPs was performed by the

Table 3: Description of the equations parameters

Parameter	Unit	Description
q_e and q_t	mg/g	The amounts of HA adsorbed per unit weight of adsorbent (adsorption capacity) at equilibrium time and time t
k_1	min^{-1}	Pseudo-first-order rate constant
k_2	g mg/min	Second-order rate constant
k_{int}	$mg/g.min^{0.5}$	Intraparticle diffusion rate constant
C	---	Intercept or Calculates the point at which a line will intersect the y-axis by using existing x-values and y-values
C_e	mg/L	Equilibrium concentration of the HA
q_{max}	g/kg	Monolayer adsorption capacity
K_b	m^3/g	Constant related to the free energy of adsorption
K_f	$(g.kg^{-1}.(gm^{-3})^n$	Freundlich capacity factor
N	---	Heterogeneity factor
$1/n$	---	Freundlich intensity parameter
C_0 and $C_{t,e}$	mg/L	the initial concentrations at the time t and equilibrium concentrations of the HA
V	L	solution volume
M	g	adsorbent dosage
D	nm	the particles size
K	---	the Debye–Scherrer constant (0.89),
λ	nm	the X-ray wavelength Cu-ka (0.15406 nm),
β	radian	the full width of the main peak at half intensity
θ	degree	the position of main peak

XRD patterns and is shown in Figure 1.

Point of Zero Charge

Figure 2 exhibits the point of zero charge (pzc) study for IOMNPs in pH value range of 2–14.

Effect of Initial pH

Figure 3 presents the effect of initial pH on the IOMNPs adsorption results at the initial 10 mg/L HA concentration.

Effect of Initial Adsorbent Dose

In this research, the influence of IOMNPs doses using an initial HA solution concentration of 10 mg/L was investigated to evaluate the adsorption capacity (q_t) [Equ. 1, Table 2] and HA removal efficiency, while the dosage of IOMNPs varied from 2 to 4 g/L. Figure 4 illustrates the effect of adsorbent dosages versus uptake percentage of HA.

Effect of Agitation Rate

The rate of HA sorption onto IOMNPS was studied using agitation rate ranging from 150 to 300 rpm and is shown in Figure 5.

Kinetic Experiments and Effect of Contact Time

The equilibrium time study (saturation point) and contact time effects were performed using kinetic experiments at the pH value of 4.5, agitation rate of 250 rpm, working HA concentrations of 10, 35, 60 and 100 mg/L and adsorbent dose of 2.7 g/L. Figure 6a and b present the effect of contact time on HA removal and adsorption capacity.

Pseudo-first-order model [Equ. 2, Table 2] was determined from the linear plots of ln (q_e - q_t) versus t for working initial HA concentrations at room temperatures (25°C). A straight-line plot of t/q_t versus t for pseudo-second-order model [Equ. 3, Table 2] also was drawn. The values of q_e, k_1, k_2 and the correlation coefficients, r^2, were calculated and are listed in Table 4.

The plots of $t^{0.5}$ vs. q_t for IDM [Equ. 4, Table 2] is depicted in Figure 7. Values of constants k_{int1} and $k_{int2,}$ which come from the slopes of the linear portions and correlation coefficients for IDM present also in Table 4.

Isotherm Experiments and Effect of Initial Concentrations of HA

Isotherm experiments were used to study the IOMNPs adsorption capacity (q_t) and adsorption removal at the HA concentrations from 10 to 100 mg/L [Figure 8a and b]. Parameters of Freundlich model [Equ. 5, Table 2] were determined with plot of log q_e versus log C_e [Figure 9a]. Also, plot of $1/q_e$ versus $1/C_e$ to analysis of data with the Langmuir model [Equ. 6, Table 2] were drawn in Figure 9b. Then, values of the constants, q_{max}, K_b and k_f, were calculated from the slop and intercept of the respective plots. The obtained parameters and correlation coefficient (r^2) of the both isotherm models are listed in Table 5.

Determine Presence of Interferences

Wavelength scans to determine the presence and influence of interferences on the UV_{abs} of the samples is shown in Figure 10.

Effect of Ionic Strength on Adsorption Experiments and Final Turbidity

The effect of ionic strength on the HA removal, adsorption capacity and turbidity at HA concentration of 10 mg/L was studied, as background electrolyte, and is summarized in Table 6.

Also, the effect of ionic strength on the adsorption experiments and turbidly at the working HA concentrations was compared in a) the solutions containing of 0.1 mol/L NaCl and b) the solutions that did not have electrolyte [Table 7].

DISCUSSION

The XRD patterns of the IOMNPs as shown in Figure 1 revealed that there were no characteristic peaks of impurities and that diffraction bands are very broad. The six characteristic peaks (88, 112, 114, 164, 174 and 454) for Fe_3O_4 marked by their indices were observed.

Relationship between peak broadening in XRD and particle size was determined via Debye–Scherrer equation.[17] The value of the IOMNPs using the Scherrer's formula [Equ. 7, Table 2] at the 454 reflection peak, $2\theta \sim 36°$ and 2.52 Å indicated the IOMNPs with approximately 37 nm in mean diameter size. This result was not complying with the data obtained from the company [60 nm in Table 1]. This may be due to different value of the NaOH solution and pH value of the solution, which plays an important role in controlling the crystal size,[17] so it can be conclude that IOMNPs have size range of 37–60 nm.

Table 4: Pseudo-first-and second-order and IDM models constants [*]

Input data		Pseudo-first-order model			Pseudo-second-order model			Intra particle diffusion model			
C_0 (mg/L)	$q_{e,exp}$ (mg/g)	K_1 (min^{-1})	$q_{e,cal}$ (mg/g)	r^2	K_2 (g/mg.min)	$q_{e,cal}$ (mg/g)	r^2	K_{1int}	r^2	K_{2int}	r^2
10	2.38	0.0008	0.76	0.55	0.02	2.28	0.992	0.169	0.905	-0.11	0.894
35	7.06	0.001	0.65	0.77	0.005	6.6	0.989	0.426	0.963	-0.58	0.955
65	14.10	0.0008	0.77	0.66	0.0038	13.55	0.995	0.774	0.991	-0.53	0.912
100	20.45	0.0008	0.77	0.58	0.0026	19.56	0.993	0.869	0.997	-0.94	0.892

[*] conditions: IOMNPs dose: 2.7 g/L, contact time: 30–420 min, agitation rate: 250 rpm and pH: 4.5

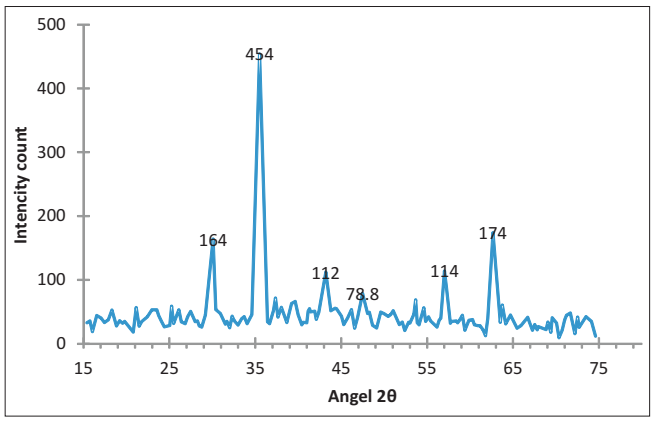

Figure 1: X-ray diffraction patterns of IOMNPs (Number above peaks indicate distance in nm between crystal planes)

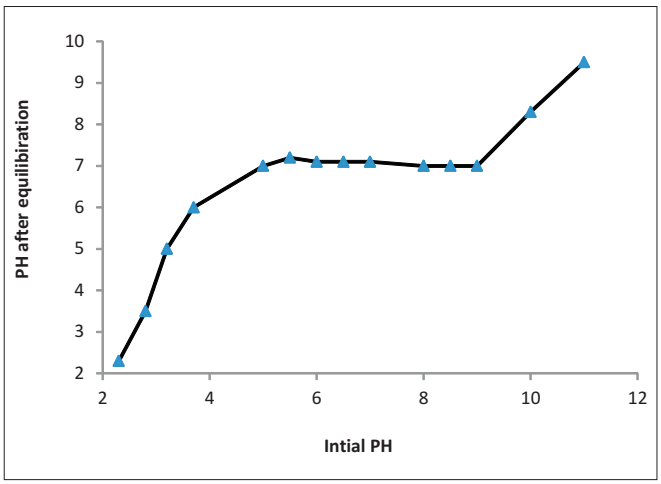

Figure 2: PZC value of IOMNPs

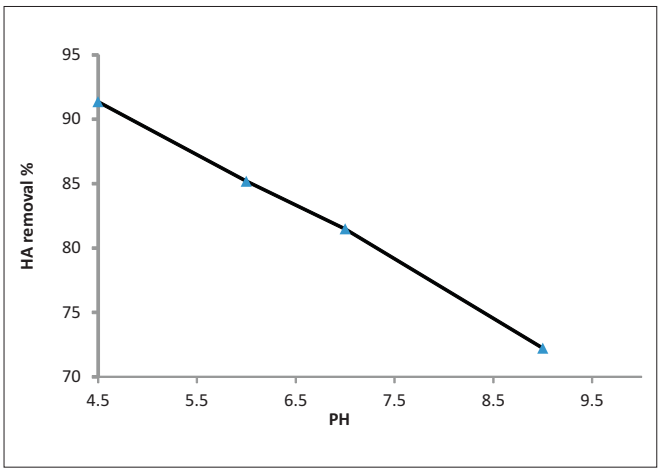

Figure 3: Effect of pH on HA removal (%)

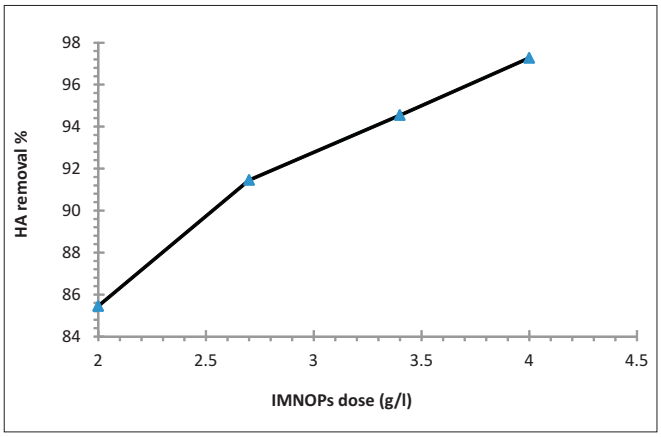

Figure 4: Effect of IOMNPs dose onto HA removal efficiency

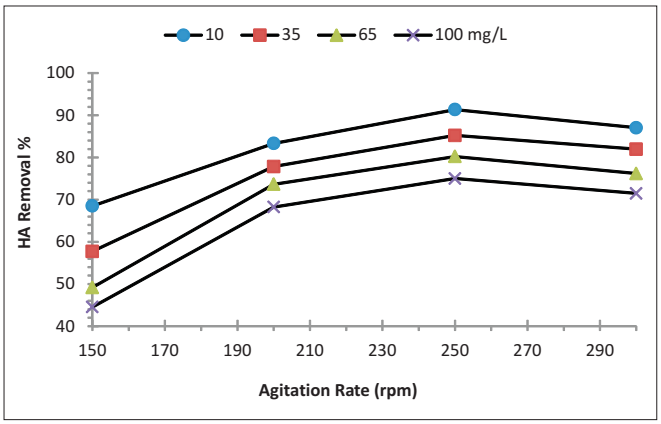

Figure 5: Effect of agitation rate onto HA removal efficiency at working HA concentrations

The chemical composition of the sample at which the zeta potential is zero is called the pzc. In this pH, the total net surface charge of the sample also is zero.[20] The pH_{pzc} of the IOMNPs used in the study was around 7 [Figure 2]. Due to using different methods in the synthesis of iron oxides nanoparticles, different values of pzc (3.8 to 9.9) were reported in the literatures.[14] Figure 3 indicates that in general, HA removal increases with decreasing initial pH values from 9 to 4.5. If the pH < pH_{pzc}, solutions produced more protons than hydroxide groups and the adsorbent surface would be positively charge (cationic) and tend to attracting anions. On the other hand, at pH > pH_{pzc}, hydroxide groups are dominant and surface of adsorbent will be negatively charge (anionic) and tend to attracting the cations.[14,21] The pK_a values of acidic sites on various humic substances are generally in the range of 3–4.5. So, if solutions have pH larger than these pK_a values, phenolic and carboxylic groups in the HA structure are ionized and HA becomes dominantly negatively charged.[12] As a result, electrostatic attraction between surfaces positive charge on IOMNPs and surface negative charge of HA increases, so the highest extents of HA uptake was obtained at pH 4.5. When pH > pH_{pzc}, both IOMNPs and HA surfaces are expected to be predominant negatively charged. Therefore, corresponding to increases of electrostatic repulsion between surfaces of HA and IOMNPs, HA removal efficiency decreases [Figure 3]. These results indicate the surface charges of both HA and IOMNPs changes, as a function of pH, and play a significant role in adsorption.

It has been reported that HA adsorption onto other adsorbents such as acid-activated Greek bentonite,[3] cross-linked chitosan - epichlorohydrin beads,[22] Cetylpyridinium bromide and modified zeolite[23] also follow similar trends. With the addition of adsorbent dose in the range of 2–4 g/L [Figure 4], the increase in the adsorption efficiency was observed from 85.45 % to 97.27 %. This can be attributed to increase in the surface area and available sites of adsorbent.[24] As a result, the greater number of HA molecules would be adsorbed onto IOMNPs and thereby the higher would be the removal percentage.

As regards to Figure 5, agitation rate of 250 rpm is the best point for adsorption experiments. Owing to the rate of film diffusion

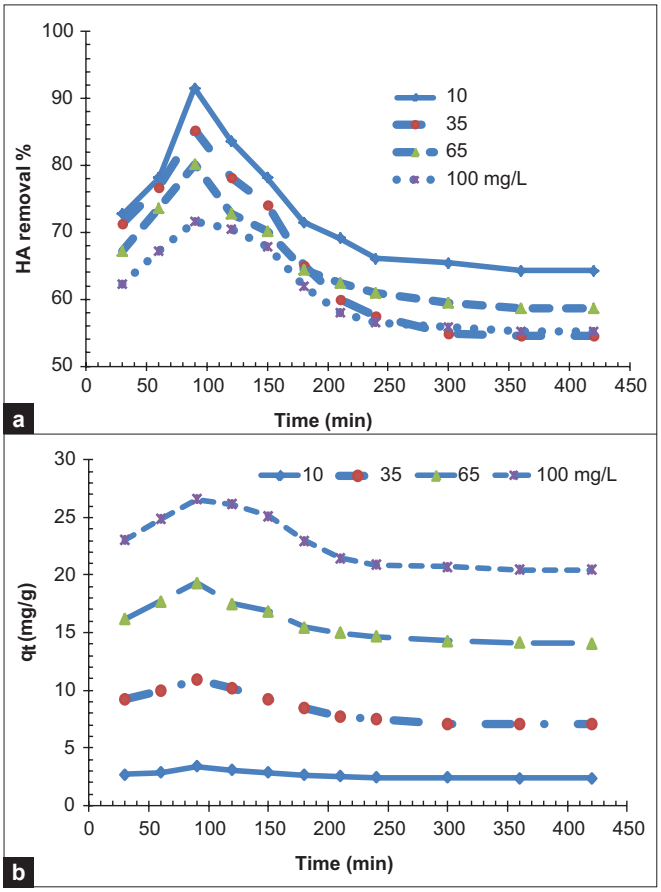

Figure 6: Effect of contact time onto (**a**) HA removal efficiency and (**b**) Adsorption capacity (q_t) of IOMNPs

Table 5: Langmuir and Freundlich isotherm constants [*]

Langmuir			Freundlich		
q_{max} (mg/g)	K_b (L/mg)	r^2	N	K_f	r^2
26.95	0.16	0.991	1.67	3.31	0.9931

[*]Conditions: HA concentration: 10–100 mg/L, IOMNPs dose: 2.7 g/L, contact time: 90 min, agitation rate: 250 rpm and pH: 4.5

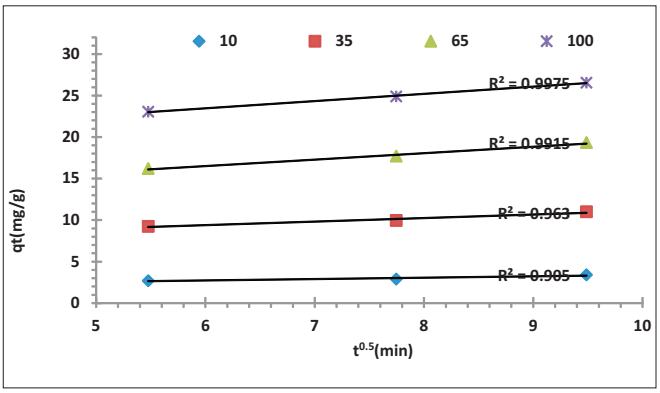

Figure 7: Intraparticle diffusion model for initial stage of experiments

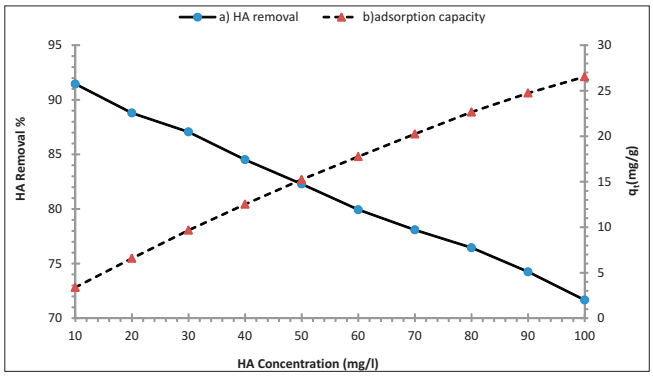

Figure 8: Effect of initial concentrations of HA onto (**a**) HA removal efficiency and (**b**) adsorption capacity (q_t) of IOMNPs

Table 6: Effect of ionic strength from 0 to 0.1(mol/L) on HA removal, turbidity production and adsorption capacity of IOMNPs[*]

Ionic strength NaCla (mol/L)	HA removal (%)	Turbidity (NTU)	Adsorption capacity (q_t)(mg/g)
0	91.52	5.6	3.39
0.005	91.98	1.2	3.41
0.02	92.90	0.97	3.44
0.04	94.44	0.91	3.50
0.07	96.91	0.86	3.59
0.1	98.77	0.81	3.66

[*] conditions: IOMNPs dose: 2.7 g/L, contact time: 90 min, agitation rate: 250 rpm, HA concentration: 10 mg/L and pH: 4.5

Table 7: Adsorption experiments and final turbidity of solutions: a) with no background electrolytes and b) with background electrolytes[*]

HA concentration (mg/L)	HA removal (%)		Turbidity (NTU)		Adsorption capacity (q_t)(mg/g)	
	a	b	a	b	a	b
10	91.52	98.77	5.6	0.81	3.39	3.66
35	85.22	90.72	12.5	1.8	11.05	11.76
65	80.23	86.91	18.8	2.5	19.31	20.92
100	75.02	80.50	26	4.1	27.78	29.81

[*] conditions: NaCl (0.1 mol/L) as background electrolytes, IOMNPs dose: 2.7 g/L, contact time: 90 min, agitation rate: 250 rpm and pH: 4.5

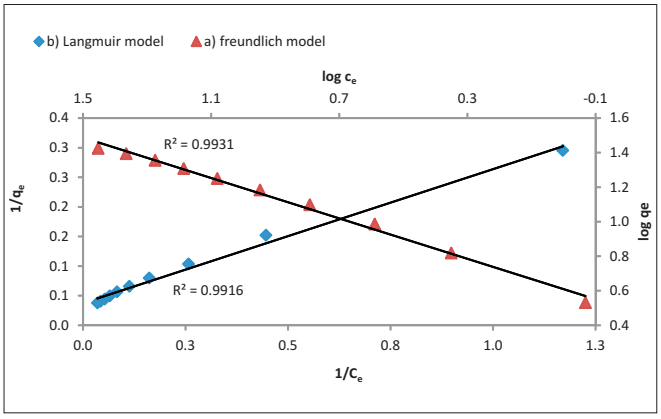

Figure 9: Linear plots of (**a**) Langmuir and (**b**) Freundlich isotherms

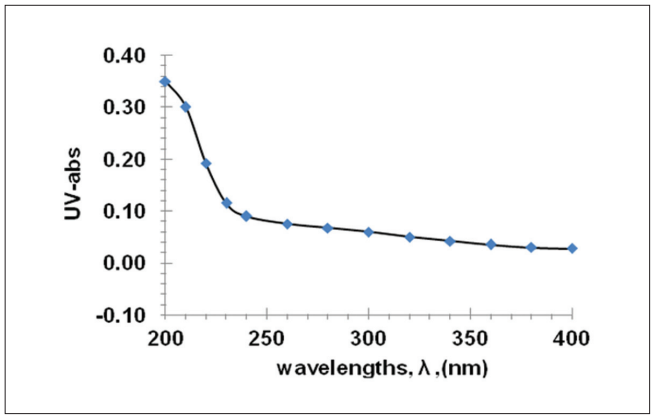

Figure 10: Wavelength scans to determine presence of interferences for treated HA solution

in this point increased and intraparticle diffusion becomes the rate-limiting step,[25] so in this condition, the adsorption process occurs faster and the equilibrium adsorption time become reduced. In the inappropriate or inadequate agitation rate, the surface film of liquid around the adsorbent will be thick and results the film diffusion to be the rate-limiting step,[25] thus the HA removal diminishes. Accordingly, agitation rate is an important factor for the film diffusion and distribution of the adsorbate and adsorbent in the bulk solution.

Regarding Figure 6, it is obvious that with increasing of contact time from 0 to 90 min, the rate of HA adsorption onto IOMNPs and the HA adsorbed per unit weight of adsorbent increases. Thus, because of that numbers of available vacant surface sites on adsorbent area are large, initially, with the passage of time, the repulsive forces between HA molecules on the solid and liquid phase increase. So, the remaining vacant surface sites are difficult to be occupied. Hence, the number of active sites available to absorb the HA molecules are limited. Consequently, HA removal and adsorption capacity diminishes.[3] This decreasing trend continued until the adsorption reached to the equilibrium point in 420 min.

Kinetic studies provide useful information from the process efficiency point of view and feasibility of scale-up operational parameters for designing economical equipments. These also are used for chemical reaction description during the period between the initial state and the final state.[21,25]

The pseudo-first-order model describes adsorption in solid–liquid systems based on the sorption capacity of solids. However, the pseudo-second-order expression has been applied for analyzing chemisorptions kinetics from liquid solutions.[18]

Referring to Table 4, it was found that correlation coefficients, r^2, for the pseudo-first-order kinetic model are relatively low and the calculated ($q_{e,cal}$)values obtained from this equation do not agree with the experimental ones)$q_{e,exp}$.,while the calculated $q_{e,cal}$ values of pseudo-second-order model were in agreement with the experimental ones at all initial HA concentrations. Consequently, pseudo-first-order kinetic model did not fit well to the whole range of HA concentrations and contact times. On the other hand, the linear plots of t/q_t versus t show a good agreement with experimental data giving the higher correlation coefficients. As a result, in the present work, pseudo-second-order kinetic model can produce better fitting to the experimental data of HA adsorption.

By increasing of the HA loadings, the value of pseudo-second-order adsorption rate constant (k_2) decreased [Table 4]. Thus, because of that the mass transfer rate of the adsorbate increases[24] from 2.38 to 20.45 mg/g. Similar conclusions have been drawn in the literature for adsorption of HA onto the other adsorbents such as acid-activated Greek bentonite[3] and chitosan-H_2SO_4 beads.[26]

The adsorption of HA to the magnetic material may be due to ligand exchange reaction between functional groups (e.g., hydroxyl and carboxylates) of HA and the surface hydroxyls of metal oxides.[14] The overall rate of adsorption include: a) Transportation of the adsorbate from the bulk phase of the solution to the surface of adsorbent, which is called film or surface diffusion, b) Transportation of the adsorbate molecules to adsorption site on the inside of the pore structure that is called intraparticle or pore diffusion, and c) Mass action or adsorption/desorption between the adsorbate and active sites.[25] Because the pseudo-second-order kinetic model cannot give a definite mechanism of adsorption,[3] IDM was employed to evaluate the rate-limiting step in adsorption process.[18] In this study, the adsorption experiments presented multi-linearity in three phase's including: i) an initial linear portion or rapid adsorption stage (contact times of 30–90 min) that represents intraparticle or pore diffusion is rate-limiting, ii) the second linear section or gradual reduction adsorption stage (90–360 min) and, iii) third section or plateau stage (> 360 min) (only the first stage was shown). Although the plots of intraparticle diffusion with a slope k_{int} are linear for the every three portions, the IDM fit the experimental data very well for initial linear portion

compared with others [Figure 7]. Nevertheless, owing to the fact that the plots are not passed from the origin, in case of HA adsorption by IOMNPs, intraparticle diffusion model is not the sole rate-limiting step.[18] Therefore, all above processes involved the rate controller but only one was rate limiting in any linear portion. Similar results were found in other papers.[3]

The plots of isotherms study revealed that corresponding to enhancing the HA loading, its uptake per unit weight of IOMNPs was increasing [Figure 8]. This may be due to increase in the mass driving force, hence allowing more HA molecules to pass from the solution to the adsorbent surface.[3] Under the same conditions, the number of reactive functional groups, which bind to the HA molecules and adsorbent surface, were diminished.[7] So, the removal efficiency of HA decreased. Consequently, the initial HA concentration plays an important role in the adsorption process.

Langmuir model usually applies to monolayer adsorption processes within a low concentration range. This model supposes that adsorption occurs on a homogeneous surface, whereas Freundlich model is suitable for high and middle concentration environments for both multilayer and monolayer adsorption processes and assumes that the adsorbent has a heterogeneous surface.[18,25]

Results showed that correlation coefficient of both isotherms are above the 0.99, ($r^2 > 0.99$), which implies favorably both of them for isotherm experiments. But in general, using the Freundlich model gives a higher correlation coefficient ($r^2 = 0.9931$) than the Langmuir model ($r^2 = 0.991$) [Figure 9 and Table 5]. So, it can be concluded that the tested IOMNPs have a heterogeneous surface with different abilities of HA adsorption. As well, the adsorption intensity factor (n) was greater than unity (n = 1.67) that indicates the favorability of the adsorption process.[22]

With regarding to Figure 10, it is obvious that there is no sharp peak or irregularities in the adsorption scan, and adsorption increases with decreasing of wavelengths. This means that there are not interferences in samples (e.g., colloidal particle, nitrate, nitrite and bromide) which influence the UV_{abs}.[19]

It is evident that an increase in the ionic strength enhanced the adsorptive efficiency of IOMNPs. An increase in ionic strength from 0 to 0.04 (mol/L) caused an increase in percentage removal of HA from 91.52 % to 94.44 %. Further increase of ionic strength from 0.04 to 0.1 mol/L resulted in an increase of removal from 94.44 % to 98.77 %. Also at similar conditions, adsorption capability of IOMNPs increased slightly from 3.39 to 3.5 and finally reached to 3.66 mg/g, respectively. Turbidity decreased from 5.6 to 0.91 NTU and eventually reached to 0.81 NTU [Table 6]. According to Table 7, generally with increasing of HA concentrations, turbidity of the treated solutions increased significantly. Results exhibited, compared with solutions that have no electrolyte background, in solutions that contain NaCl, adsorption capacity of IOMNPs and HA removal increased and turbidity decreased [Table 7].

The increase of HA adsorption with an increase in ionic strength may be explained by several mechanisms: a) with increasing ionic strength, solubility of HA molecules diminishes. As a result mass transfer of HA from the solution phase to the solid phase increases; b) Molecular volume of HA due to minimizing the electrostatic repulsion between ionized oxygen groups decreases. Hence, the penetration capability of HA molecules from the pores becomes greater, which enhances the HA removal, and c) In accordance with ion strength increasing, the electrical double layer becomes more compact, which causes the particles and adsorbate molecules to become closer together.[3,27]

Results of this study revealed that HA molecules can produce turbidity in aquatic solutions, which is proportional to its loading rate [Tables 5 and 6]. In fact, increasing of ionic strength, corresponding to the above mechanisms, can accelerate the HA removal from solution. So, dispersion of HA molecules in solution will decrease and HA content in solution and pursuant turbidity decreases. Proper interpretation of this reduction by ionic strength was not found in other similar articles. So, it is suggested to do more research about this field.

CONCLUSIONS

Kinetic and isotherm experiments were conducted for the adsorption of HA from aqueous solutions onto IOMNPs. Results revealed that the adsorption isotherm was fitted well by Freundlich model and followed the pseudo-second-order model. Meanwhile, the intraparticle diffusion was found to fit well with the initial portion than the other, but it was not the sole rate-determining step. It is obvious that with increase of HA loading, adsorption capacity of IOMNPs increased and HA removal diminished, but at above condition, the turbidity of treated solutions increased. With increasing of ionic strength, HA removal efficiency was increased and turbidity of treated solutions was reduced. With decreasing of the pH value, increasing the dose of IOMNPs and agitation rate to 250 rpm, the HA removal efficiency onto IOMNPs was decreased.

ACKNOWLEDGMENT

This article is the result of MSc. thesis approved in the Isfahan University of Medical Sciences (IUMS). The authors wish to acknowledge to Vice Chancellery of Research of IUMS for the financial support, Research Project, # 390251.

REFERENCES

1. Jones MN, Bryan ND. Colloidal properties of humic substances. Adv Colloid Interface Sci 1998;78:1-48.
2. Ghosh K, Schnitzer M. Macromolecular structures of humic substances. Soil Sci 1980;129:266.
3. Doulia D, Leodopoulos C, Gimouhopoulos K, Rigas F. Adsorption of humic acid on acid-activated Greek bentonite. J Colloid Interface Sci 2009;340:131-41.
4. Chang E, Chao SH, Chiang PC, Lee JF. Effects of chlorination on THMs formation in raw water. Toxicol Environ Chem 1996;56:211-25.
5. Imyim A, Prapalimrungsi E. Humic acids removal from water by aminopropyl functionalized rice husk ash. J Hazard Mater 2010;184:775-81.
6. Peng X, Luan Z, Chen F, Tian B, Jia Z. Adsorption of humic acid onto pillared bentonite. Desalination 2005;174:135-43.
7. Liang L, Luo L, Zhang S. Adsorption and desorption of humic and fulvic acids on SiO2 particles at nano- and micro-scales. Colloids Surf A Physicochem Eng Asp 2011;384:126-30.
8. Giasuddin ABM, Kanel SR, Choi H. Adsorption of humic acid onto nanoscale zerovalent iron and its effect on arsenic removal. Environ Sci Technol 2007;41:2022-7.
9. Balcke GU, Kulikova NA, Hesse S, Kopinke FD, Perminova IV, Frimmel FH. Adsorption of humic substances onto kaolin clay related to their structural features. Soil Sci Soc Am J 2002;66:1805-12.
10. Anirudhan T, Ramachandran M. Surfactant-modified bentonite as adsorbent for the removal of humic acid from wastewaters. Appl Clay Sci 2007;35:276-81.
11. Shen YF, Tang J, Nie ZH, Wang YD, Ren Y, Zuo L. Preparation and application of magnetic Fe3O4 nanoparticles for wastewater purification. Sep Purif Technol 2009;68:312-9.
12. Bekaroglu S, Yigit N, Karanfil T, Kitis M. The adsorptive removal of disinfection by-product precursors in a high-SUVA water using iron oxide-coated pumice and volcanic slag particles. J Hazard Mater 2010;15;183:389-94.
13. Vermeer A, Van Riemsdijk W, Koopal L. Adsorption of humic acid to mineral particles. 1. Specific and electrostatic interactions. Langmuir 1998;14:2810-9.
14. Illés E, Tombácz E. The role of variable surface charge and surface complexation in the adsorption of humic acid on magnetite. Colloids Surf A Physicochem Eng Asp 2003;230:99-109.
15. Faraji M, Yamini Y, Rezaee M. Extraction of trace amounts of mercury with sodium dodecyle sulphate-coated magnetite nanoparticles and its determination by flow injection inductively coupled plasma-optical emission spectrometry. Talanta 2010;81:831-6.
16. Liu J, Zhao Z, Jiang G. Coating Fe3O4 magnetic nanoparticles with humic acid for high efficient removal of heavy metals in water. Environ Sci Technol 2008;42:6949-54.
17. Kim D, Zhang Y, Voit W, Rao K, Muhammed M. Synthesis and characterization of surfactant-coated superparamagnetic monodispersed iron oxide nanoparticles. J Magn Magn Mater 2001;225:30-6.
18. Boparai HK, Joseph M, O'Carroll DM. Kinetics and thermodynamics of cadmium ion removal by adsorption onto nano zerovalent iron particles. J Hazard Mater 2010;186:458-65.
19. Eaton AD, Franson MAH, editors. Standard methods for the examination of water and wastewater. Amer Public Health Assn; Washington, DC: USA; 2005.
20. Lyklema J, editor. Fundamentals of interface and colloid science. Waltham, Massachusetts: Academic Press; 2005; 12-4.
21. Walter J, Weber J, editors. Physico chemical process for water quality control. Hoboken, New Jersey: John Wiley and Sons Inc; 1972; 640 Pages.
22. Wan Ngah WS, Hanafiah MAKM, Yong SS. Adsorption of humic acid from aqueous solutions on crosslinked chitosan-epichlorohydrin beads: Kinetics and isotherm studies. Colloids Surf B Biointerfaces 2008;65:18-24.
23. Zhan Y, Zhu Z, Lin J, Qiu Y, Zhao J. Removal of humic acid from aqueous solution by cetylpyridinium bromide modified zeolite. J Environ Sci 2010;22:1327-34.
24. Moussavi G, Talebi S, Farrokhi M, Sabouti RM. The investigation of mechanism, kinetic and isotherm of ammonia and humic acid co-adsorption onto natural zeolite. Chem Eng J 2011;171:1159-69.
25. Benefield LD, Judkins JF, Weand BL, editors. Process chemistry for water and wastewater treatment. Fonte: Englewood Cliffs; Prentice Hall Inc; 1982.
26. Ngah WSW, Fatinathan S, Yosop NA. Isotherm and kinetic studies on the adsorption of humic acid onto chitosan-H2SO4 beads. Desalination 2011;272:293-300.
27. Peng X, Luan Z, Zhang H. Montmorillonite–Cu (II)/Fe (III) oxides magnetic material as adsorbent for removal of humic acid and its thermal regeneration. Chemosphere 2006;63:300-6.

Source of Support: Isfahan University of Medical Sciences, **Conflict of Interest:** None declared.